

Precision studies of v_n fluctuations

Tyler Gorda¹ and Paul Romatschke¹

¹*University of Colorado Boulder, Boulder, CO*

(Dated: May 25, 2022)

Abstract

The power spectrum of heavy ion collisions is investigated by studying initial state fluctuations on top of a smooth hydrodynamic flow. In particular, the stability of the location of the first minimum of the power spectrum and the dependence of the hydrodynamic response v_n/ε_n on n and on η/s are discussed. In our study we develop a new Green's function method for the analytic hydrodynamic flow by S. Gubser and make use of a fully non-linear hydrodynamics code. We find that there will be no well-defined first minimum of the response for $n < 10$, due to the fact that all minima in that region are found to be sensitive to the location of the initial perturbations. Also, we find that the often proposed form of the hydrodynamical response, that $\ln(v_n/\varepsilon_n)$ depend quadratically on n and linearly on η/s , should not hold once many events have been averaged over.

I. INTRODUCTION

Experiments at the Relativistic Heavy Ion Collider (RHIC) and the Large Hadron Collider (LHC) have both been able to produce and detect an exotic phase of matter, the quark-gluon plasma (QGP), by colliding massive nuclei at relativistic energies. The energy densities involved in these collisions are so intense that the hadrons participating in the collisions dissolve into their constituent partons, creating a state of matter in which the color charge is no longer confined. Despite the short lifetime of this matter (on the order of $10 \text{ fm}/c$), there is strong evidence that it has time to (locally) thermalize and can be described as a nearly perfect fluid. One can compute the expected abundance of different particle species produced from a thermalized QGP and compare it with the ratios of detected particle species at RHIC or LHC; the results are in good agreement with one another [1], [2]. Another place where hydrodynamics has provided particularly good agreement with heavy ion experiments is with the so-called "collective flow" [1] [3]. When two nuclei collide the resulting QGP will be anisotropic in space, because of differences in density distributions inside the individual nuclei, even for central collisions. Within hydrodynamics (implying strong interactions), pressure gradients will convert this spatial anisotropy into an anisotropy in momentum space. This effect would not be observed if the matter produced were noninteracting.

The full power spectrum resulting from heavy ion collisions is given by the Fourier Transform of the two particle correlation function [4]

$$\frac{dN}{d\Delta\phi} = \left\langle \frac{dN}{d\Delta\phi} \right\rangle \left(1 + 2 \sum_{m=1}^{\infty} |v_m|^2 \cos(m\Delta\phi) \right). \quad (\text{I.1})$$

Here N is the particle count and $\Delta\phi$ is the relative momentum angle between two observed particles. The elliptic flow is controlled by the coefficient v_2 . From this power spectrum, one should be able to extract information about the initial density

fluctuations or other physics in the QGP, in analogy with the Cosmic Microwave Background power spectrum.

One way to theoretically investigate this power spectrum is by studying hydrodynamic fluctuations on top of a smooth fluid flow and following how these perturbations propagate through to the particle spectra and on to the v_m . This approach was taken by Staig and Shuryak in a series of research papers [3] [5] [6] studying linear perturbations. One can also study the power spectrum numerically using fully nonlinear hydrodynamic codes.

Both of these approaches require much analytic or numerical effort to obtain the power spectrum. In order to obviate the need for this extensive effort every time one wants to compare theory and experiment, focus has been placed on determining how particular features of the power spectrum are affected by properties of the QGP itself, e.g. the viscosity or freezeout temperature. Particular interest has been placed on the first minimum of the power spectrum [6] or on the hydrodynamic response of the system v_m/e_m where the e_m , defined by

$$e_m = \left| \frac{\int r^m \varepsilon(x) e^{im\phi} d^2x}{\int r^m \varepsilon(x) d^2x} \right|, \quad (\text{I.2})$$

are the initial state eccentricities. Here $\varepsilon \propto T^4$ is the initial energy density, and the integrals are over the transverse plane of the collision. This response is often proposed to depend on hydrodynamic parameters by

$$\ln \left(\frac{v_m}{e_m} \right) \propto -\frac{4}{3RT} m^2 \frac{\eta}{s}, \quad (\text{I.3})$$

where R is the transverse size of the collision, T is the temperature of the collision, η is the shear viscosity, and s is the entropy density. This dependence of the response has been investigated by Lacey *et al.* [7]. One of the questions we investigate in this paper is how robust these conclusions are; that is, can information about the initial

state fluctuations or about properties of the QGP actually be extracted once one has averaged over many events?

A. Analytically Known Flows: Bjorken and Gubser Flow

Full, nonlinear hydrodynamic flow generally requires computer code in order to generate results, because the full equations are too complicated to solve analytically. However, one can often investigate the approximate behavior of the full solutions by considering small perturbations around a known analytical flow. If one possesses a given analytical flow, i.e. its energy-momentum tensor $T_0^{\mu\nu}$, then one can consider energy momentum tensors of the form

$$T^{\mu\nu} = T_0^{\mu\nu} + \delta T^{\mu\nu}, \quad (\text{I.4})$$

where $\delta T^{\mu\nu}$ is small to the first order. Taking the covariant derivative of this perturbed energy-momentum tensor leads directly to the first order equations for the perturbation. In what follows we will consider perturbations to the energy density, pressure, and four velocity directly, which make up the energy momentum tensor

$$T^{\mu\nu} = (\varepsilon + p)u^\mu u^\nu + p g^{\mu\nu} - 2\eta \sigma^{\mu\nu} - \zeta (\nabla_\gamma u^\gamma) \Delta^{\mu\nu} \quad (\text{I.5})$$

where ε is the energy density, p is the pressure, u^μ is the four-velocity, $g_{\mu\nu}$ is the metric, η is the shear viscosity, ζ is the bulk viscosity and

$$\sigma^{\mu\nu} = \Delta^{\alpha\mu} \Delta^{\beta\nu} \left(\frac{\nabla_\alpha u_\beta + \nabla_\beta u_\alpha}{2} - \frac{g_{\alpha\beta}}{3} \nabla_\gamma u^\gamma \right), \quad (\text{I.6})$$

$$\Delta^{\mu\nu} = u^\mu u^\nu + g^{\mu\nu}. \quad (\text{I.7})$$

The simplest flow used to model heavy ion collisions is the so-called Bjorken flow, which possesses boost invariance in the longitudinal z direction (the velocity profile

is such that a Lorentz boost in the z direction leaves the flow unchanged), rotational invariance in the transverse plane (the ϕ direction), and translational invariance in the transverse plane. What makes this flow so simple is that by the change of coordinates from (t, x, r, ϕ) to (τ, η, r, ϕ) defined by

$$t = \tau \cosh \eta \quad z = \tau \sinh \eta \quad (\text{I.8})$$

the four-velocity profile reduces to $u^\mu = (1, 0, 0, 0)$ with a metric

$$ds^2 = -d\tau^2 + \tau^2 d\eta^2 + dr^2 + r^2 d\phi^2. \quad (\text{I.9})$$

In the past few years another analytical flow has been found that can be used to model heavy ion collisions. Gubser [8], [9] exchanged the translational invariance in the transverse plane associated with Bjorken flow for conformal invariance. This allows the fluid to expand radially at the expense of fixing the trace of the energy-momentum tensor to be zero. Having a radially-expanding analytical fluid flow opens up the possibility of investigating more realistic linear perturbations than were permitted by Bjorken flow. In what follows, we shall refer to this new flow as Gubser flow.

There exists a coordinate system in which Gubser flow is also particularly simple. First, one can rescale the metric

$$ds^2 = \tau^2 d\hat{s}^2. \quad (\text{I.10})$$

Introducing the parameter q , which characterizes the transverse scale of the system (more precisely, q^{-1} does this), and the new coordinates ρ and θ defined by

$$\sinh \rho = -\frac{1 - q^2 \tau^2 + q^2 r^2}{2q\tau}, \quad (\text{I.11})$$

$$\tan \theta = \frac{2qr}{1 + q^2 \tau^2 - q^2 r^2}, \quad (\text{I.12})$$

one can complete the transformation. The rescaled metric in the coordinates $(\rho, \eta, \theta, \phi)$ is given by

$$d\hat{s}^2 = -d\rho^2 + d\eta^2 + \cosh^2\rho(d\theta^2 + \sin^2\theta d\phi^2), \quad (\text{I.13})$$

and the fluid flow is simply $\hat{u}^\mu = (1, 0, 0, 0)$. Note that because the Gubser flow is conformal, $\zeta = 0$, $\varepsilon = 3p$, and $\varepsilon \propto T^4$.

In what follows we first examine rapidity independent perturbations of the Gubser flow. We begin by discussing first order perturbations to the Gubser flow in general, and then state the specific setup that we have examined. We then present our two approaches to the problem. We state our results for this analysis, and compare them with previous work along these lines. After this semi-analytic approach, we examine similar perturbations numerically in full nonlinear hydrodynamics. The power spectra we obtain are analyzed, specifically for the stability of the first minimum and for the dependence of the hydrodynamic response on η/s . These results are stated and the results of the two approaches are compared in a concluding section.

II. η -INDEPENDENT PERTURBATIONS OF THE GUBSER FLOW

We begin by outlining the general framework of first order perturbations to the Gubser flow. As derived in [8], the background temperature in the rescaled frame is given by

$$\hat{T}_b = \left(\frac{\hat{T}_0}{(\cosh \rho)^{2/3}} + \frac{h \sinh^3 \rho}{9(\cosh \rho)^{2/3}} {}_2F_1 \left(\frac{3}{2}, \frac{7}{6}; \frac{5}{2}; -\sinh^2 \rho \right) \right), \quad (\text{II.1})$$

where $h = \eta/T^3$, $\hat{T} = \tau 11^{1/4} T$, ${}_2F_1$ is a hypergeometric function, and here and in everything that follows, $q = (4.3 \text{ fm})^{-1}$. This value was used by Gubser [8] [9] as the value that best matched experimental results at RHIC. The parameter \hat{T}_0

characterizes the initial temperature of the flow. The perturbation is implemented by varying the rescaled temperature and four-velocity by a small amount:

$$\hat{T} = \hat{T}_b(1 + \delta), \quad (\text{II.2})$$

$$\hat{u}_\mu = \hat{u}_{0\mu} + \hat{u}_{1\mu}, \quad (\text{II.3})$$

where $\hat{u}_{0\mu} = (-1, 0, 0, 0)$ is the covariant components of the background four-velocity and

$$\hat{u}_{1\mu} = (0, 0, u_\theta(\rho, \theta, \phi), u_\phi(\rho, \theta, \phi)), \quad (\text{II.4})$$

$$\delta = \delta(\rho, \theta, \phi). \quad (\text{II.5})$$

As detailed in [9] we can further split the spacial variables from the timelike one by projecting the scalar δ onto the basis of spherical harmonics and the two nonzero components of the $\hat{u}_{1\mu}$ onto the derivatives of the spherical harmonics using the decomposition

$$\delta = \sum_{L,M} c_{LM} \delta_L(\rho) Y_{LM}(\theta, \phi), \quad (\text{II.6})$$

$$\hat{u}_{1i} = \sum_{L,M} c_{LM} v_L(\rho) \partial_i Y_{LM}(\theta, \phi), \quad (\text{II.7})$$

with $i \in \{\theta, \phi\}$. Here, the c_{LM} are simply the coefficients in these expansions (the ambiguity in their definition can be removed by demanding that $\delta_L(\rho_0) = 1$ for some fixed ρ_0). In our analysis, we include all $L \leq 25$. We will often drop the L subscript and simply write δ and v when there is an equation that holds for each L . Note that we are ignoring the so-called vector modes by making this decomposition, for the most general basis for vectors on S^2 depending on the coordinates (ρ, θ, ϕ) will be of the form

$$v_i(\rho, \theta, \phi) = v_s(\rho) \partial_i S(\theta, \phi) + v_v(\rho) V_i(\theta, \phi), \quad (\text{II.8})$$

where S is a scalar function and the divergence of V on S^2 vanishes [9]. The equations for δ and v can be written in the form

$$\frac{d\vec{w}}{d\rho} = -\mathbf{\Gamma} \cdot \vec{w}, \quad (\text{II.9})$$

where $\vec{w} = (\delta, v)$ and the components of the $\mathbf{\Gamma}$ matrix are

$$\Gamma_{11} = \frac{h \tanh^2 \rho}{3\hat{T}_b}, \quad (\text{II.10})$$

$$\Gamma_{12} = \frac{L(L+1)}{3\hat{T}_b \cosh^2 \rho} \left(h \tanh \rho - \hat{T}_b \right), \quad (\text{II.11})$$

$$\Gamma_{21} = \frac{2h \tanh \rho}{h \tanh \rho - 2\hat{T}_b} + 1, \quad (\text{II.12})$$

$$\Gamma_{22} = \frac{8\hat{T}_b^2 \tanh \rho + h\hat{T}_b \left(\frac{-4(3L(L+1)-10)}{\cosh^2 \rho} - 16 \right) + 6h^2 \tanh^3 \rho}{6\hat{T}_b \left(h \tanh \rho - 2\hat{T}_b \right)}. \quad (\text{II.13})$$

This matrix equation (II.9) can be reduced to a second order equation for δ :

$$\frac{d^2\delta}{d\rho^2} + \frac{d\delta}{d\rho} \left(\Gamma_{11} - \frac{1}{\Gamma_{12}} \frac{d\Gamma_{12}}{d\rho} + \Gamma_{22} \right) + \delta \left(\frac{d\Gamma_{11}}{d\rho} - \frac{\Gamma_{11}}{\Gamma_{12}} \frac{d\Gamma_{12}}{d\rho} + \Gamma_{11}\Gamma_{22} - \Gamma_{12}\Gamma_{21} \right) = 0. \quad (\text{II.14})$$

All of the information about the perturbed system follows from the solutions of (II.14).

We have used (II.14) to investigate the evolution of an initial Gaussian hotspot

$$\delta(\rho_0, \theta, \phi) \propto \exp \left(- \frac{\theta^2 + \theta_0^2 - 2\theta\theta_0 \cos(\phi - \phi_0)}{2s^2} \right), \quad (\text{II.15})$$

with the further assumption that there be no initial velocity perturbations.

$$\hat{u}_i(\rho_0) = 0, \quad i \in \{\theta, \phi\}. \quad (\text{II.16})$$

We have done this in two separate ways (method A and method B), which we will outline in the next two subsections. The r_0 coordinate was varied, keeping $\tau_0 = 1$ fm

fixed for the hotspot. This fixed a value for ρ_0 by the coordinate relations (I.11), (I.12). A standard Cooper-Frye isothermal freezeout was then used in order to compute the particle spectrum of pions:

$$E \frac{dN}{d^3p} = - \int d\Sigma_\mu p^\mu f \left(\frac{p^\nu u_\nu}{T} \right). \quad (\text{II.17})$$

The distribution function f was taken to be a simple Boltzmann distribution. Modifications of the freezeout surface were taken into account by keeping terms in the exponent of the Boltzmann distribution to the first order in $\delta\tau(r, \phi)$, the modification to the freezeout time. After obtaining the particle spectrum, we calculated two-particle correlations by multiplying two single particle distributions and averaging over the ϕ component of the initial perturbation

$$\frac{dN}{d(\Delta\phi)} = \int \frac{dN}{d(\phi_1 - \psi)} \frac{dN}{d(\phi_2 - \psi)} d\psi, \quad (\text{II.18})$$

with $\Delta\phi = \phi_1 - \phi_2$. The two-particle distributions were then Fourier decomposed in order to generate a power spectrum; that is, the coefficients $|v_m|^2$ in the expansion

$$\frac{dN}{d\Delta\phi} = \left\langle \frac{dN}{d\Delta\phi} \right\rangle \left(1 + 2 \sum_{m=1}^{\infty} |v_m|^2 \cos(m\Delta\phi) \right). \quad (\text{II.19})$$

A. First approach: Standard initial value problem

The first method that we used to solve (II.14) was by using a standard numerical ordinary differential equation solver. The initial conditions were set for each of the L equations by decomposing the initial hotspot (II.20) into spherical harmonics. These components were then set to be the coefficients c_{LM} in (II.6), and the initial condition for each δ was then simply $\delta_L(\rho_0) = 1$. The second initial condition was fixed by the demand that there be no initial fluid flow. This is the approach followed in work by Staig and Shuryak [6].

B. Second approach: The Green's Function Method

There is a completely different way to approach the initial value problem described above. Consider a flow in which a perturbation “turns on” at an initial time ρ_0 .

$$T^{\mu\nu} = T_0^{\mu\nu} + \theta(\rho - \rho_0)\delta T^{\mu\nu}. \quad (\text{II.20})$$

Here $T^{\mu\nu}$ is the total energy-momentum tensor for the system. This leads to hydrodynamic equations of the form

$$\nabla_\mu T^{\mu\nu} = \delta T^{\mu\nu} \partial_\mu \theta(\rho - \rho_0), \quad (\text{II.21})$$

We can thus view an initial value problem for the hydrodynamic equations as a problem of a *sourced* fluid flow for δ . With this application in mind, we shall now outline how we construct the relevant Green's functions for this problem.

Observe that the Γ s in (II.14) can be viewed as functions of $\tanh \rho$ only. This means that we can rewrite the equation in terms of the new variable $x \equiv \tanh \rho$. If we further expand (II.14) to first order in h , we arrive at

$$\begin{aligned} (1-x^2)^2 \delta''(x) - \frac{2}{3}x(1-x^2)\delta'(x) + \frac{1}{3}L(L+1)(1-x^2)\delta(x) + \\ + \frac{h}{3T_0}(1-x^2)^{2/3} \left[\left(x \left(\frac{2}{1-x^2} \right) - 2xL(L+1) \right) \delta(x) + \right. \\ \left. + 3(L(L+1)(1-x^2) + 3x^2 - 1) \delta'(x) \right] = 0, \end{aligned} \quad (\text{II.22})$$

Now observe that for $\rho \in (-\infty, \infty)$, we have $x \in (-1, 1)$. This suggests that perhaps the ansatz

$$\delta(x) = \sum_{n=1}^{\infty} a_n P_n(x), \quad (\text{II.23})$$

with P_n the n th Legendre polynomial and a_n the n th unknown coefficient, will be useful. If we substitute (II.23) into (II.22) and then apply the integral operator

$\int_{-1}^1 dx P_m(x)$ to both sides of the equation, we arrive at an algebraic relation between the unknown coefficients a_i . Unfortunately, in the case $h \neq 0$ these relations involve an infinite number of the a_i . If, however, we limit our ansatz to a finite expansion

$$\delta(x) = \sum_{n=1}^N a_n P_n(x), \quad (\text{II.24})$$

we arrive at a set of linear relations between the coefficients $\{a_n : n \in [0, N] \cap \mathbb{N}\}$. In our analysis, we take $N = 50$, when solving the linear equations, but we only use the first 25 terms when calculating results. We use a larger N when solving the linear equations than when generating results because truncating the series introduces errors, which mainly affect the larger n coefficients. If we regard this set as a column vector a and the set of matrix coefficients in the resulting linear equations M , then we have reduced our original differential equation (II.14) to the linear equations

$$Ma = 0. \quad (\text{II.25})$$

For each L in (II.14), there should be two linearly independent solutions. We can find them by considering the two “initial conditions”

$$(a_0, a_1) = (1, 0) \quad \text{or} \quad (a_0, a_1) = (0, 1). \quad (\text{II.26})$$

In the inviscid case, these correspond to even and odd solutions respectively. These initial conditions can be implemented as follows. If we split the column vector a as

$$a = (a_{ic} | \bar{a}) \quad (\text{II.27})$$

and the matrix M as

$$M = (M_1 | M_2), \quad (\text{II.28})$$

where a_{ic} is one of the two initial conditions, \bar{a} are the $(N - 2)$ remaining coefficients, M_1 is a $(N - 2) \times 2$ matrix and M_2 is a square $(N - 2) \times (N - 2)$ matrix. We then

see that (II.25) can be rewritten as $M_1 a_{ic} + M_2 \bar{a} = 0$, which allows one to solve for the unknown coefficients

$$\bar{a} = (-M_2^{-1} M_1) a_{ic}. \quad (\text{II.29})$$

We now address the question of the source. Suppose we have a sourced hydrodynamic system with evolution equation

$$\nabla_\mu T^{\mu\nu} = J^\nu. \quad (\text{II.30})$$

How does this source J^ν propagate through to the equation for δ (II.14)? Recall that δ was defined by

$$\hat{T} = \hat{T}_b(1 + \delta), \quad (\text{II.31})$$

We can perform a similar decomposition to this source term as was done with the δ/v decomposition; that is

$$J^\nu = \sum_{LM} (J_L^\rho Y_{LM}, J_L^A \partial^i Y_{LM}), \quad i \in \{\theta, \phi\}. \quad (\text{II.32})$$

Using this decomposition, one finds that the source term on the right side of (II.14) is

$$\left(\Delta'_1 - \frac{\Gamma'_{12}}{\Gamma_{12}} \Delta_1 + \Gamma_{22} \Delta_1 \right) J_L^\rho - \Delta_2 \Gamma_{12} J_L^A + \Delta_1 (J_L^\rho)', \quad (\text{II.33})$$

where

$$\Delta = \left(\frac{1}{4\hat{T}_b^4}, \frac{3}{2\hat{T}_b^3(2\hat{T}_b - h \tanh \rho)} \right). \quad (\text{II.34})$$

Using this source and the method described above, one can construct solutions of sourced hydrodynamic equations in the $(\rho, \eta, \theta, \phi)$ coordinate system. We have applied this method to the problem outlined above, and our results are described in the following sections. This method is also interesting in its own right and can be used to analyze two point functions directly, as has been investigated by Springer

and Stephanov [10]. Letting $j(x)$ denote the source of the δ equation (II.14), we can write a particular L solution in the form

$$\delta(x) = \delta_{\text{hom}}(x) + \int_{x_0}^x dx' G(x, x') j(x') \quad (\text{II.35})$$

with

$$G(x, x') = \frac{\Theta(x - x')}{W[f_L, f_R](x')} \sum_a \sum_b (l_a r_b - l_b r_a) P_a(x') P_b(x). \quad (\text{II.36})$$

Here, δ_{hom} is a solution to the homogeneous, unsourced equation, Θ is the Heaviside step function, and $W[f_L, f_R]$ is the Wronskian of the solutions f_L and f_R that satisfy the left and right boundary conditions of interest. They have the expansions

$$f_L(x) = \sum_a l_a P_a(x) \quad \text{and} \quad f_R(x) = \sum_a r_a P_a(x) \quad (\text{II.37})$$

respectively. Since we have constructed the actual Green's functions, we can investigate the true two point functions for a Dirac- δ source using this method.

III. RESULTS

We have calculated the power spectrum for a first order perturbation using method B for $\hat{T}_0 = 7.9$, which corresponds to an initial temperature of $T_0 = 500$ MeV. The sample inviscid plot is shown in Figure 1. The width of the Gaussian hotspot used in our analysis was $s = 0.2$, to make it significantly more narrow than the background flow representing the colliding nuclei. Viscous plots looked qualitatively similar and have not been included, for we have followed Staig and Shuryak [6] in ignoring viscous corrections to the spectrum.

In Figure 1 we see that the position of the first minimum of the power spectrum is not stable to changes in the initial radial position of the perturbation r_0 . Increasing r_0 tends to shift the first minimum of the power spectrum to larger m values. We

observe the minimum to vary by two or three harmonics, which is broadly consistent with Staig and Shuryak [6]. In what follows, however, we note a number of differences between their work and ours (see, in particular the following two subsections III A and III B). It seems reasonable to conclude that the first minimum of the fixed p_T differential power spectrum is not a stable observable, even in linear hydrodynamics. If one were to average over many events with multiple perturbations, there would not be a well-defined location of this first minimum. Since real hydrodynamics is nonlinear, it seems doubtful that there will be a detectable first minimum to the fixed p_T differential power spectrum in real heavy ion collision data.

Let us briefly digress in order to perform an error analysis of our method. There are two main sources of numerical error: a Riemann sum was used in the integration process and the freezeout surface was truncated at the edge in order to not need to access times $\rho < \rho_0$ (see the comparison subsection below for a discussion of this). The Riemann sum error was estimated by performing sums with two different

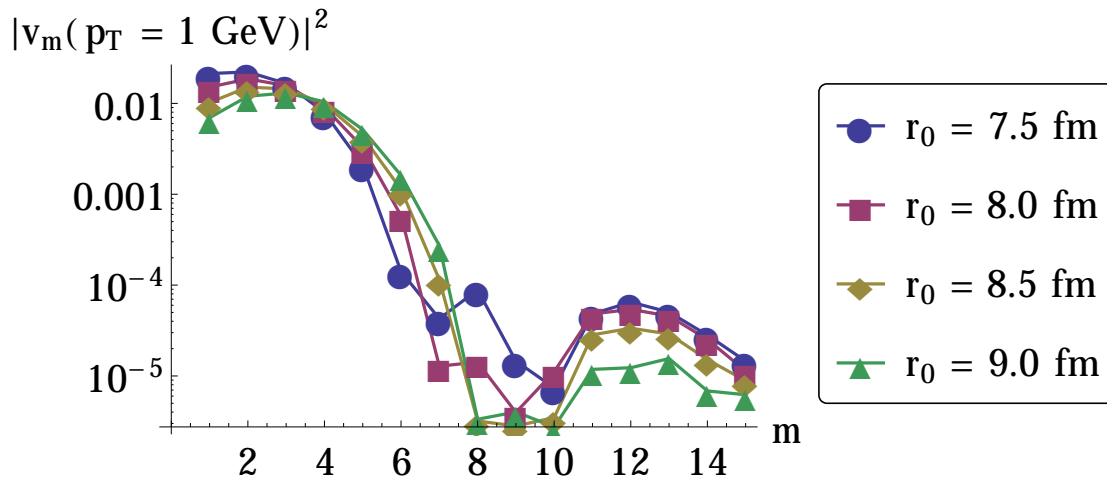


FIG. 1: Fixed $p_T = 1$ GeV differential power spectrum for $\eta = 0$. Numerical error is smaller than the symbol size.

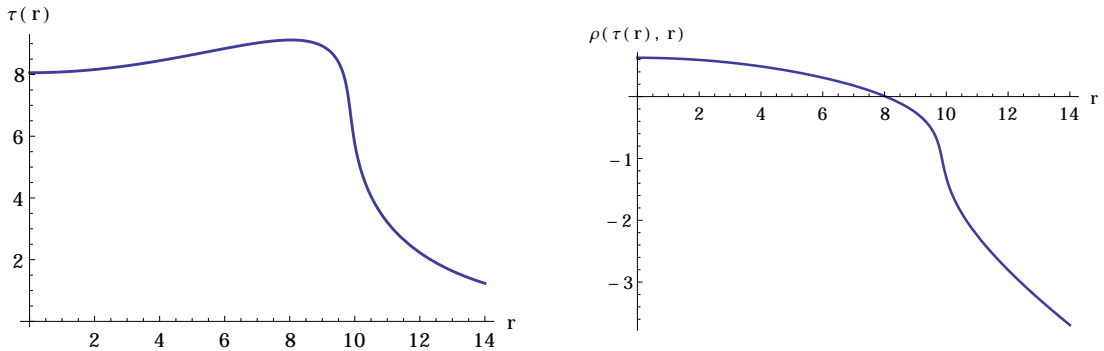


FIG. 2: Left: a plot of the freezeout surface for $T_0 = 630$ MeV. Right: the ρ values corresponding to this freezeout surface.

resolutions; and the error associated with the truncation of the freezeout surface was estimated by varying where this truncation was made, calculating the changes to the power spectra, and then extrapolating these changes to the edge of the freezeout surface. The total error was found to be 2 – 3%, in the region plotted in Figure 1, with the larger errors associated to the minima of the power spectra.

We have also tried to identify potential systematic errors in our study and found one issue that needs to be taken into account. First, recall that the Gubser timelike coordinate ρ is not the same as the physical proper time τ . From the coordinate transformations (I.11), (I.12) one sees that the coordinate ρ depends on both of the physical coordinates τ and r . This means that for a given freezeout surface there is a restricted range of ρ_0 that one must choose from in order to avoid needing information about the flow *before* the perturbation is initialized (when calculating the Cooper-Frye freezeout integral (II.17), for example). Figure 2 illustrates this effect. On the left, the freezeout surface for $T_0 = 630$ MeV is plotted. On the right, the value of the coordinate ρ is shown for the points on the freezeout surface. We see that if we wish to avoid freezing out for $\rho < \rho_0$ at the edge of the freezeout surface, we must either choose a ρ_0 sufficiently early, or only integrate out to a certain r in the Cooper-Frye

formula (II.17); that is, ignore parts of the freezeout surface. Since we wish to fix the τ_0 coordinate of our perturbation to be 1 fm, this leads to the necessary choice of ignoring the very edge of the freezeout surface. In order to keep this systematic error small, we chose to cut the freezeout surface between $r = 12.3$ fm and $r = 12.6$ fm in order to include as much of the features of the surface as possible. This allowed us to choose the r_0 value of the perturbation to be anything larger than about 8 fm (or, for $T_0 = 500$ MeV, about 7.5 fm). This is a rather large value, but bringing it closer to the center would have necessitated ignoring significant portions of the freezeout surface, and in turn would result in a large systematic error of our procedure.

A. Remarks on differences from previous works

Staig and Shuryak [6] have analyzed the same problem that we have outlined above as an initial value problem. In their paper, they found that the first minimum of the fixed p_T differential power spectrum did not shift more than one harmonic as they varied the r_0 position between 3 fm and 5.5 fm, and the overall shape of the power spectra remained consistent as the coordinate was varied. Despite the broadly consistent shape of the differential power spectra between our work and theirs, there are some subtle differences in analysis. For this reason, we highlight here the few differences between our analysis and that of Staig and Shuryak.

Staig and Shuryak presumably evaluated the full Cooper-Frye integral (II.17) with a saddle point approximation, where the integrand was evaluated at the maximum of the background exponent. In our analysis, we found that the integrand in the Cooper-Frye expression (II.17) was not sharply peaked for every value of ϕ_P , the momentum angular coordinate, so a full calculation of the particle spectra was necessary. We evaluated the integral in full, using only a Riemann sum in the r coordinate; our numerical errors due to this sum were discussed above.

We also used a smaller value of \hat{T}_0 than Staig and Shuryak. They chose to use $\hat{T}_0 = 10.1$, corresponding to an initial temperature of $T_0 = 630$ MeV, in order to allow more time to evolve before freezeout. This changes the detailed shape of the power spectra, and shifts the peaks and minima somewhat, but it does not change our qualitative conclusion that the first minimum is not stable under variations in the initial coordinate r_0 of the hotspot.

Finally, there is no mention in Staig and Shuryak's work of the systematic error introduced related to the cutting of the freeze-out surface (see our discussion above). Note, however, that they used values of r_0 that necessitate cutting a large portion of the freezeout surface to avoid freezing out for $\rho < \rho_0$.

B. Hydrodynamic response of the Gubser flow

In this section we study the linear hydrodynamic response to the perturbations by calculating the ratio v_m/e_m where e_m are the initial eccentricities. Again, for the initial eccentricities, we have used the normalization

$$e_m = \left| \frac{\int r^m \varepsilon(x) e^{im\phi} d^2x}{\int r^m \varepsilon(x) d^2x} \right|, \quad (\text{III.1})$$

where here $\varepsilon \propto T^4$ is the initial energy density, and the integrals are over the transverse plane of the collision. The hydrodynamic response of the system is frequently characterized by the ratio v_m/e_m . We have calculated this ratio; in particular we have calculated it for integrated v_m over the p_T range 0 – 2 GeV. This was performed with the weighting

$$v_m^{(\text{integrated})} = \frac{\int dp_T p_T v_m(p_T) \frac{dN}{dp_T}}{\int dp_T p_T \frac{dN}{dp_T}}, \quad (\text{III.2})$$

where the integrals are over 0 – 2 GeV. Our results for the inviscid case are plotted in Figure 3. The temperature of the fluid and width of the perturbation are identical to what was used in the corresponding plots above.

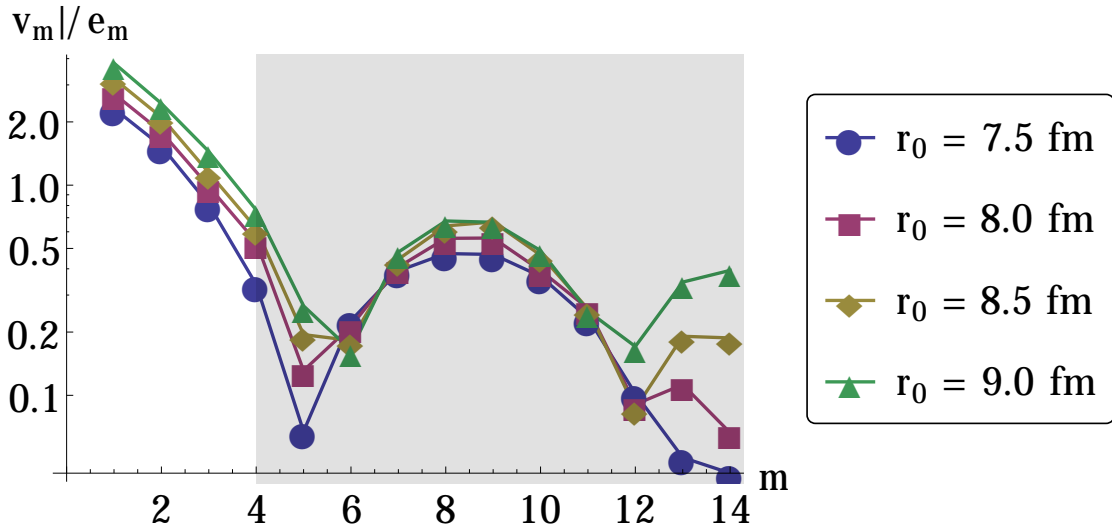


FIG. 3: Inviscid response. Numerical error is smaller than the symbol size. The shaded region $m > 3$ is cutoff-dependent.

We note here that the e_m are ill-defined for the Gubser flow, for $\varepsilon_0(r)$, the background energy density, exhibits a power law decay. From the background temperature profile (II.1), we find the leading order behavior

$$\varepsilon_0(r) \propto r^{-16/3} + \dots \quad (\text{III.3})$$

Since the background energy density is independent of the azimuthal angle ϕ and the perturbation is a Gaussian, we have that the numerators of the expression for e_m are finite for every m . On the other hand, the denominators diverge for large enough m , for they are given by

$$\int^R r^m (r^{-16/3} + \dots) r dr \propto R^{(m-10/3)} + \dots \rightarrow \infty \quad (\text{III.4})$$

if $m > 3$. In order to remedy this, we have imposed a cutoff on the volume by only integrating to a finite r_{max} . This cutoff, however, artificially causes the response to

scale with r_{\max} as

$$\frac{v_m}{e_m} \propto (r_{\max})^{m-10/3} + \dots \quad (\text{III.5})$$

for $m > 3$. This consideration must be held in mind when examining the hydrodynamical response of the Gubser flow. To aid with this, we have shaded the cutoff-dependent region in Figure 3.

IV. CALCULATING THE v_m USING NUMERICAL HYDRODYNAMICS

Using the Gubser flow to model the energy density profile of the quark gluon plasma after a heavy ion collision was useful because it provided an analytical flow on which to do linear perturbations. However, it was not without its drawbacks. The Gubser flow was conformal, whereas the flow in a real heavy ion collision is not, and there were limitations on where the original perturbation could be placed. The latter difficulty necessitated discarding small pieces of the freezeout surface in the Cooper-Frye integral (II.17). Finally, real viscous hydrodynamics is inherently nonlinear, whereas the Gubser analysis above only involved linear perturbations. With these shortcomings in mind, we have conducted analysis of the v_m coefficients using numerical hydrodynamics.

The specific code used was the Causal Viscous Hydro Code for Non-Central Heavy Ion Collisions version 0.5.2 by Luzum and Romatschke [11]. On top of the central collision background energy density used in the code, a Gaussian of width $s = 0.5$ fm and height 0.125 GeV^4 was added, again, so that the perturbation would be localized relative to the background energy density. Figure 4 shows the integrated response over the p_T range $0 - 4$ GeV of a system with $\eta/s = 0.08$ as the initial radial position of the perturbation is varied between $2 - 6$ fm. The curves representing perturbations with smaller r_0 are truncated at smaller m . This is because smaller r_0 leads to smaller v_m and e_m , which the code could not accurately calculate with

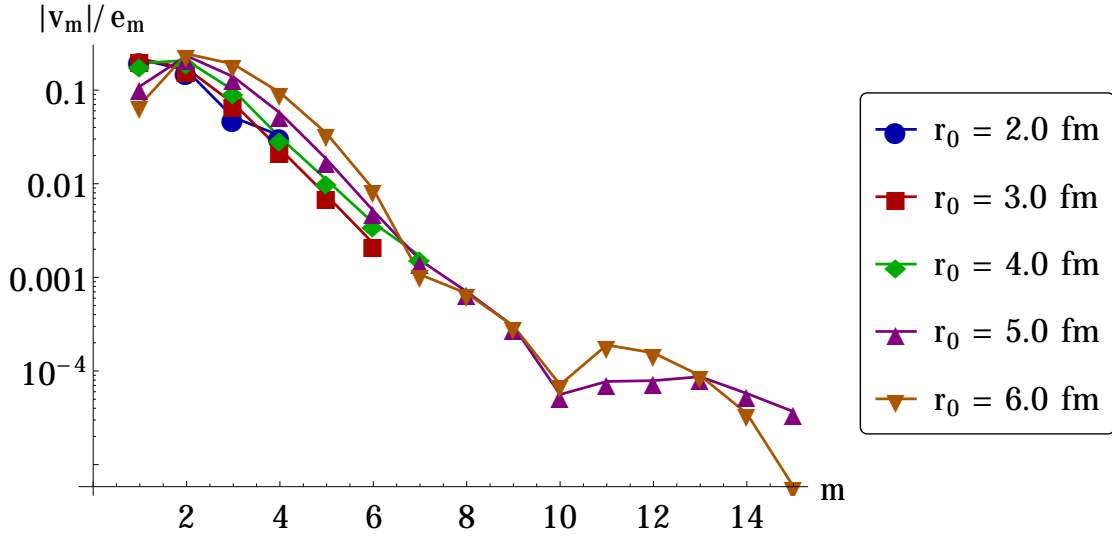


FIG. 4: Response in non-linear hydrodynamics. Here $\eta/s = 0.08$. Errors are no larger than the symbol size.

feasible lattice spacings. We did, however, run codes for multiple lattice spacings in order to get a sense of the errors. We have only plotted those points that have errors smaller than the symbol size on the plots.

From Figure 4 there does not appear to be a well-defined minimum until at least $m = 10$, except perhaps for the perturbation farthest from the symmetry axis. After averaging over many events with many initial perturbation locations, one would not expect to find a minimum for $m < 10$, which makes it doubtful that experiments would be able to detect one.

With this observation in mind, we turn to examining the proposed form for the response

$$\ln\left(\frac{v_m}{e_m}\right) \propto -\frac{4}{3RT}m^2\frac{\eta}{s}, \quad (\text{IV.1})$$

to see whether numerical hydrodynamics supports this simple dependence on η/s .

Figure 5 shows plots of v_m/e_m for $\eta/s = 0.08, 0.16, 0.24,$ and 0.32 for perturbations

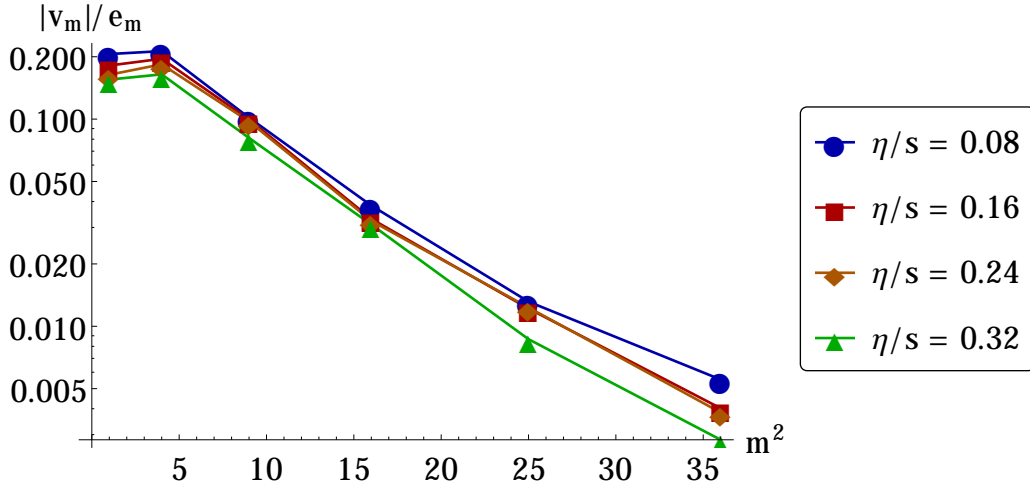


FIG. 5: Hydrodynamic response for different values of η/s . Note that this is a log plot and that the horizontal axis is m^2 . Here, $r_0 = 4$ fm. Errors are no larger than the symbol size.

centered at 4 fm from the beamline. As expected, we see that v_2 decreases as η/s increases. We note here, however, that there is not a noticeable change in slope as η/s is varied, already placing strain on the proposed linear dependence. For each value of η/s we have fit $\ln(v_m/e_m)$ to the form

$$A + Bm^2, \quad (\text{IV.2})$$

the proposed form of the response (IV.1). Since the coefficients B are proposed to depend linearly on η/s , we show in Figure 6 a linear fit to these $(\eta/s, B)$ values for the $r_0 = 4$ fm and the $r_0 = 6$ fm cases. For each value of viscosity over entropy density, we plot the B value for the finest lattice spacing with error bars equal in size to the difference between the B values for the finest and second finest lattice spacings (most of which are too small to be seen on the plot).

The $A + Bm^2$ form was found to fit the logarithm of the response for each vis-

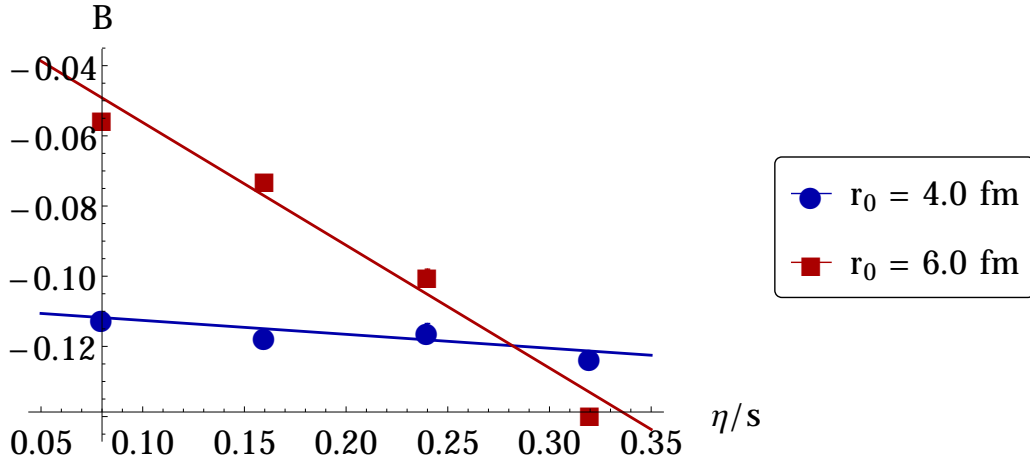


FIG. 6: Fit of the coefficients of m^2 in quadratic fits of $\ln(v_m/e_m)$ (cf. (IV.1)). Each individual fit of $\ln(v_m/e_m)$ includes the values $m = 2$ to $m = 6$. Errors are smaller than the symbol size.

cosity over entropy ratio well, but we see from Figure 6 that as the position of the perturbation is varied, the slope of the best fit line changes dramatically. It would thus seem from this work that after many events are averaged over one would no longer expect to see this dependence of the response (IV.1) on m and η/s .

V. CONCLUSIONS

We have used semi-analytical and numerical methods to investigate the hydrodynamical response of a heavy ion collision system with initial state perturbations. Semi-analytically, using the Gubser flow, we found that the first minimum of the response was sensitive to the location of the initial-state perturbation. Moreover, this minimum was located in a region where the initial state eccentricities were ill-defined. Numerically, we found that there did not appear to be a well-defined first minimum in the region $m < 10$. Taking these results together, we conclude that in

the region $m < 10$, which includes the region accessible by experiment, there should not occur a sharp minimum of the response. Furthermore, our investigations do not support the dependence of the measured response on m and η/s as

$$\ln\left(\frac{v_m}{e_m}\right) \propto -m^2 \frac{\eta}{s}, \quad (\text{V.1})$$

for the slope in the linear fits of $\ln(v_m/e_m)$ vs. η/s varies with the location of the initial perturbation. In addition, for some locations, the linear dependence is not even observed. We thus find that many of the features thought to contain information about the medium will be washed out when averaging over many event locations, or at the very least they will be modified substantially.

We have also described a method for calculating the Green's functions for the η -independent, linearized Gubser flow to first order in h . This would allow one to examine the true two-point functions of this system at central rapidity. The method could also in principle be extended to remove the central rapidity restriction.

VI. ACKNOWLEDGEMENTS

This work was supported by the Sloan Foundation, Award No. BR2012-038, and the DOE, Award No. DE-SC0008132. We thank Pilar Staig and Edward Shuryak for an illuminating correspondence and J. Nagle for fruitful discussions.

-
- [1] P. Sorensen, arXiv:nucl-ex/1201.0784v1. 2
 - [2] P. Braun-Munzinger, K. Redlich, J. Stachel, arXiv:nucl-th/0304013v1. 2
 - [3] E. Shuryak, Phys. Rev. **C80**, 054908 (2009). 2, 3
 - [4] A. P. Mishra, R. K. Mohapatra, P. S. Saumia, A. M. Srivastava, Phys. Rev. **C77**, 064902 (2008). 2

- [5] P. Staig, E. Shuryak, Phys. Rev. **C84**, 034908 (2011). 3
- [6] P. Staig, E. Shuryak, Phys. Rev. **C84**, 044912 (2011). 3, 9, 13, 14, 16
- [7] R. A. Lacey, A. Taranenko, J. Jia, D. Reynolds, N. N. Ajitanand, *et al.* Phys. Rev. Lett. **112**, 082302 (2014). 3
- [8] S. S. Gubser, Phys. Rev. **D82**, 085027 (2010). 5, 6
- [9] S. S. Gubser, A. Yarom, Nucl. Phys. **B846**, 469-511 (2011). 5, 6, 7, 8
- [10] T. Springer, M. Stephanov, Nucl. Phys **A904-905**, 1027c, (2013), arXiv:1210.5179v1 [nucl-th]. 13
- [11] M. Luzum and P. Romatschke, Phys. Rev. **C78**, 034915 (2008) 19